

Table 1: Vertical excitation energies and dominant contributions of the  $S_0$  and  $S_1$  states of fulvene optimized with SA2-CASSCF(6,6)/6-31G and MRCI(CAS(6,6))/6-31G. For MRCI, the Pople correction is also given (MRCI/+Pople).

State	$\Delta E$ (eV)	Configuration	%
SA2-CASSCF(6,6) – $S_0$ optimization			
$S_0$	0.000	$(1b2)^2(2b2)^2(3b2)^0(4b2)^0$ $(1a2)^2(2a2)^0$	75.7
$S_1$	4.080	$(1b2)^2(2b2)^2(3b2)^1(4b2)^0$ $(1a2)^1(2a2)^0$ $(1b2)^2(2b2)^1(3b2)^2(4b2)^0$ $(1a2)^1(2a2)^0$	72.0 14.8
SA2-CASSCF(6,6) – $S_1$ optimization			
$S_0$	1.403	$(1b2)^2(2b2)^2(3b2)^0(4b2)^0$ $(1a2)^2(2a2)^0$ $(1b2)^2(2b2)^1(3b2)^1(4b2)^0$ $(1a2)^2(2a2)^0$	65.4 13.8
$S_1$	2.630	$(1b2)^2(2b2)^2(3b2)^1(4b2)^0$ $(1a2)^1(2a2)^0$ $(1b2)^2(2b2)^1(3b2)^2(4b2)^0$ $(1a2)^1(2a2)^0$	70.8 16.1
SA2-CASSCF(6,6) – MXS optimization			
$S_0$	2.932	$(19a)^2(20a)^2(21a)^1(22a)^1(23a)^0(24a)^0$ $(19a)^2(20a)^1(21a)^1(22a)^2(23a)^0(24a)^0$	71.7 15.5
$S_1$	2.932	$(19a)^2(20a)^2(21a)^2(22a)^0(23a)^0(24a)^0$ $(19a)^2(20a)^1(21a)^2(22a)^1(23a)^0(24a)^0$	58.6 16.9
MRCI – $S_0$ optimization			
$S_0$	0.000/0.000	$(1b2)^2(2b2)^2(3b2)^0(4b2)^0$ $(1a2)^2(2a2)^0$	69.0
$S_1$	3.907/3.779	$(1b2)^2(2b2)^2(3b2)^1(4b2)^0$ $(1a2)^1(2a2)^0$	70.1
MRCI – $S_1$ optimization			
$S_0$	1.268/1.194	$(1b2)^2(2b2)^2(3b2)^0(4b2)^0$ $(1a2)^2(2a2)^0$ $(1b2)^2(2b2)^1(3b2)^1(4b2)^0$ $(1a2)^2(2a2)^0$	61.8 10.5
$S_1$	2.638/2.600	$(1b2)^2(2b2)^2(3b2)^1(4b2)^0$ $(1a2)^1(2a2)^0$ $(1b2)^2(2b2)^1(3b2)^2(4b2)^0$ $(1a2)^1(2a2)^0$	67.3 10.8

---

MRCI – MXS optimization

---

$S_0$

$S_1$

---

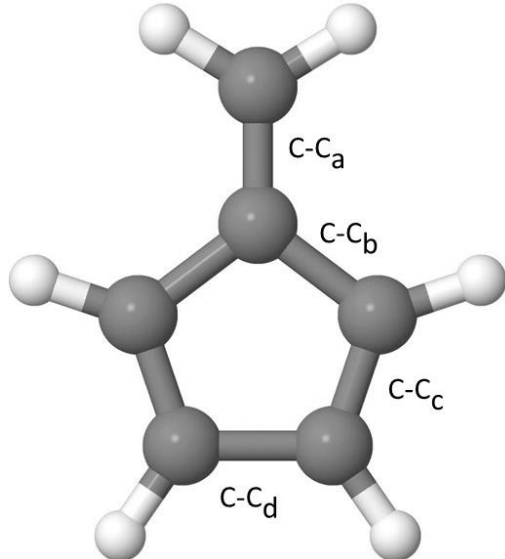
Table 2: Total energies in Hartree of fulvene

	$S_0$	$S_1$
SA2-CASSCF(6,6)- $S_0$ opt	-230.64459	-230.49466
SA2-CASSCF(6,6)- $S_1$ opt	-230.59303	-230.54794
SA2-CASSCF(6,6)-MXS-planar	-230.53683	-230.53683
MRCI- $S_0$ opt	-231.07035	-230.92677
MRCI+Q- $S_0$ opt	-231.14743	-231.00857
MRCI- $S_1$ opt	-231.02375	-230.97340
MRCI+Q- $S_1$ opt	-231.10356	-231.05189
MRCI-MXS-planar		

Table 3: Oscillator strength of the  $S_0$  to  $S_1$  transition of fulvene optimized with SA2-CASSCF(6,6)/6-31G\* and MRCI(CAS(6,6))/6-31G.

Method	$f$
SA2-CASSCF(6,6) – $S_0$ optimization	0.00
SA2-CASSCF(6,6) – $S_1$ optimization	0.00
MRCI – $S_0$ optimization	0.01
MRCI – $S_1$ optimization	0.00

Table 4: C-C bond distances of the optimized  $S_0$ ,  $S_1$ , and crossing seam structures using the SA2-CASSCF(6,6)/6-31G and MRCI(CAS(6,6))/6-31G methods.



	C-C <sub>a</sub>	C-C <sub>b</sub>	C-C <sub>c</sub>	C-C <sub>d</sub>
SA2-CASSCF(6,6)				
$S_0$	1.352	1.479	1.360	1.482
$S_1$	1.497	1.402	1.475	1.363
MXS	1.583	1.373	1.538	1.321
MRCI				
$S_0$	1.358	1.489	1.369	1.493
$S_1$	1.495	1.413	1.482	1.375
MXS				

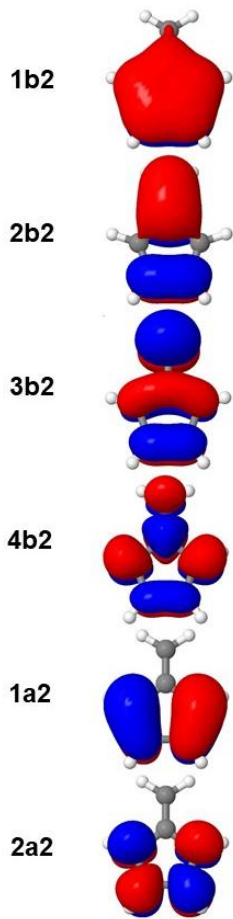


Figure 1: Optimized active orbitals for the  $S_0$  optimized with SA2-CASSCF(6,6)/6-31G.

Directories on CCR:

	SA2-CASSCF(6,6)/6-31G
S <sub>0</sub> opt	/user/ub2037/fulvene/S0-CAS
S <sub>1</sub> opt	/user/ub2037/fulvene/S1-CAS
MXS	/user/ub2037/fulvene/MXS-CAS/mxs_opt
S <sub>0</sub> opt	/user/ub2037/fulvene/S0-CI
S <sub>1</sub> opt	/user/ub2037/fulvene/S1-CI
MXS	